Available online at www.sciencedirect.com
ScienceDirect
Journal of Solid State Chemistry 181 (2008) 724–729
JOURNAL OF SOLID STATE CHEMISTRY
www.elsevier.com/locate/jssc

Synthesis of $Gd_3PO_7:Eu^{3+}$ nanospheres via a facile combustion method and optical properties

Ye Jin[a,b], Weiping Qin[c,*], Jisen Zhang[a], Xianmin Zhang[a,b], Yan Wang[a,b], Chunyan Cao[a,b]

[a]*Key Laboratory of Excited State Processes, Changchun Institute of Optics, Fine Mechanics and Physics, Chinese Academy of Science, Changchun 130033, PR China*
[b]*Graduate School of Chinese Academy of Sciences, Beijing 100039, PR China*
[c]*State Key Laboratory on Integrated Optoelectronics, College of Electronic Science and Engineering, Jilin University, 2699 Qianjin Street, Changchun 130012, PR China*

Received 27 October 2007; received in revised form 3 January 2008; accepted 7 January 2008
Available online 12 January 2008

Abstract

Eu^{3+}-doped Gd_3PO_7 nanospheres with an average diameter of ~300 nm and a narrow size distribution have been prepared by a facile combustion method and structurally characterized by X-ray diffraction and field emission scanning electron microscopy. The luminescent properties were systemically studied by the measurement of excitation/emission spectra, and emission spectra under different temperatures, as well as by photostability. The strong red-emission intensity peaking at 614 nm originates the $^5D_0 \rightarrow {}^7F_2$ transition and is observed under 254-nm irradiation, indicating that Eu^{3+} ions in Gd_3PO_7 mainly occupied non-centrosymmetry sites. The CIE1931 XY chromaticity coordinates of $Gd_3PO_7:Eu^{3+}$ nanospheres are ($x = 0.654$, $y = 0.345$) in the red area, which is near the National Television Standard Committee standard chromaticity coordinates for red. Thus, $Gd_3PO_7:Eu^{3+}$ nanospheres may be potential red-emitting phosphors for PDP and Xe-based mercury-free lamps.

Keywords: $Gd_3PO_7:Eu^{3+}$; Nanosphere; Fluorescence

1. Introduction

In order to improve the screen resolution, rare-earth phosphors in nanoscale have been investigated in recent years due to their promising technological applications in flat panel displays [1–3]. Among red phosphors in nanometer, $Y_2O_3:Eu^{3+}$ and $YBO_3:Eu^{3+}$ have attracted much attention for the applications under ultraviolet excitation [4,5]. $Y_2O_3:Eu^{3+}$ in nanometer is an efficient red phosphor, but it is not as bright under vacuum ultraviolet excitation [6]. $YBO_3:Eu^{3+}$ nanopowder presents strong absorption and high fluorescence efficiency under vacuum ultraviolet excitation. However, the characteristic emission of $YBO_3:Eu^{3+}$ is composed of almost equal contributions from the $^5D_0$–$^7F_1$ and the $^5D_0$–$^7F_2$ transitions, which gives rise to an orange-red emission instead of deep red. Thus, the low color purity hampers its applications in displays [7]. Therefore, it is urgent to develop novel red-emitting phosphors with improved color purity for applications such as plasma display panels (PDP) and field emission displays (FED).

In this paper, we report a novel red phosphor, $Gd_3PO_7:Eu^{3+}$ nanospheres, with high color purity (CIE values: $x = 0.654$, $y = 0.345$) for the first time [8]. The nanospheres with an average diameter of ~300 nm and a narrow size distribution have been prepared by a simple combustion method. It is known that phosphors with uniform small-size spheres are highly desired in developing luminescent devices because they can improve luminescent performance and screen packing [9,10]. So far, many methods have been developed to control the morphology of nanomaterials, such as the hydrothermal method [11], the template method [12,13], etc. Here, a facile combustion method was employed to manufacture the spherical nanoparticles. The strong red-emitting intensity peaking

*Corresponding author. Fax: +86 431 85168240.
E-mail address: wpqin@jlu.edu.cn (W. Qin).

0022-4596/$ - see front matter © 2008 Elsevier Inc. All rights reserved.
doi:10.1016/j.jssc.2008.01.013

at 614 nm originates the $^5D_0 \rightarrow {}^7F_2$ transition and is observed under 254-nm irradiation, indicating that Eu^{3+} ions in Gd_3PO_7 mainly occupied non-centrosymmetry sites. The investigation of emission spectra under different temperatures as well as photostability demonstrates the excellent stability, which is very suitable for applications under ultraviolet excitation.

2. Experimental section

2.1. Sample preparation

Eu^{3+}-doped Gd_3PO_7 nanospheres were synthesized by a combustion method that resembled the method for synthesizing oxides [14], but here $(NH_4)_2HPO_4$ was added to offer phosphorus. All the starting materials were of analytical grade. Solid-state $Gd_{1-x}Eu_x(NO_3)_3$ was obtained from Gd_2O_3, Eu_2O_3 and dilute HNO_3. Meanwhile, $(NH_4)_2HPO_4$ and glycin were dissolved in dilute HNO_3. The ratio of $Gd(NO_3)_3$ to $(NH_4)_2HPO_4$ was controlled accurately to prevent the formation of other phases during the combustion process. To obtain precursor solution, solid-state $Gd_{1-x}Eu_x(NO_3)_3$ was added into the mixed solution of $(NH_4)_2HPO_4$ and glycin with vigorous stirring. Then, the precursor solution was concentrated by heating until excess water evaporated and spontaneous ignition occurred. The combustion was self-propagating until glycin and nitrate were depleted. Now, the resultant Gd_3PO_7:Eu^{3+} nanospheres were obtained. The reaction was carried out in a wide-mouth beaker for a few seconds. The glycin was oxidized by nitrate ions and served as a fuel for the propellant reaction. The synthesis reaction is

$$24Gd_{1-x}Eu_x(NO_3)_3 + 20NH_2CH_2COOH + 3O_2 + 8(NH_4)_2HPO_4 \rightarrow 8Gd_{3(1-x)}Eu_{3x}PO_7 + 36N_2 + 36NO_2 + 40CO_2 + 86H_2O$$

The particle sizes of the resultant powder are quite related to the combustion flame temperature, which can be controlled by adjusting the glycin-to-nitrate ratio (G/N) [14]. Here, the glycin-to-nitrate ratio was adjusted from 1.2:1 to 1.8:1. To improve the crystallinity, the as-prepared Gd_3PO_7:Eu^{3+} nanopheres were annealed at 900 °C for 2 h.

2.2. Measurements

The crystal structure of the nanospheres was investigated by X-ray diffraction (XRD) using a Cu target radiation source ($\lambda = 1.5406$ Å). The grain size and morphology of the composite were obtained using a Hitachi S-4800 scanning electron microscope (SEM) equipped with an energy-dispersive X-ray spectrum (EDX). Excitation and emission spectra were recorded at room temperature with a Hitachi F-4500 spectrophotometer equipped with a 150-W continuous wave (CW) Xenon lamp. In the experiments investigating spectral change induced by UV light irradiation, the monochromic light dispersed from the same Xenon lamp was used as the irradiation source, with a passing band of 2.5 nm. To measure the temperature dependence of fluorescence, the annealed sample was placed in a liquid nitrogen cycling system and it was excited by a 325-nm CW He–Cd laser. The fluorescence spectra were recorded by a UV-Lab Raman Infinity (made by Jobin Yvon Company) with a resolution of 2 cm^{-1}.

3. Results and discussion

3.1. Characterization

To confirm the crystal structure of the nanospheres, XRD patterns were measured. Fig. 1 shows the XRD patterns of annealed Gd_3PO_7:Eu^{3+} nanospheres. The peak positions and intensities agree well with a bulk Gd_3PO_7 sample and indicate that annealed Gd_3PO_7:Eu^{3+} nanospheres are a monoclinic phrase according to the PDF card (JCPDS File No. 34-1066). By applying the Debye–Scherrer formula to the full-width at half-maximum of the (326) diffraction peak, the mean crystallite size was estimated to be 40 nm.

Figs. 2a–c are SEM images of the samples before (a) and after annealing (b, c), providing further insight into the morphology and microstructure of Gd_3PO_7:Eu^{3+} nanospheres. Fig. 2a is a typical image of the as-prepared sample, from which it can be seen that most grains have a spherical morphology and their average diameter is about 300 nm. The amplified image in the inset reveals that the nanosphere is the aggregation of smaller particles or crystallites (~10 nm). After annealing, the nanosphere sizes increased to about 350 nm (Fig. 2b) with more rough surfaces and the crystallites grow up to ~40 nm (Fig. 2c). Fig. 2d is the energy-disperse X-ray (EDX) spectrum taken

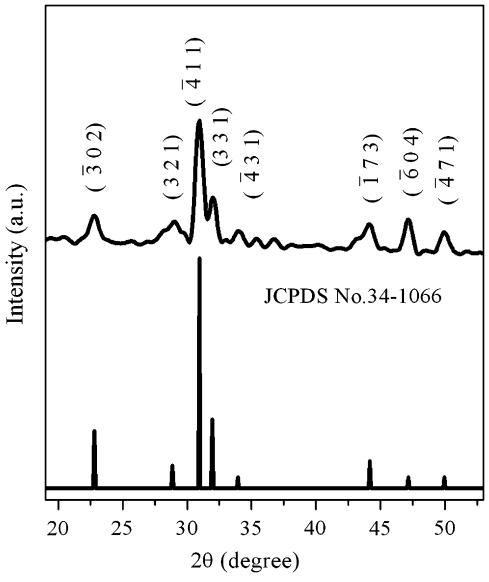

Fig. 1. XRD patterns of Gd_3PO_7:Eu^{3+} nanospheres annealed at 900 °C for 2 h.

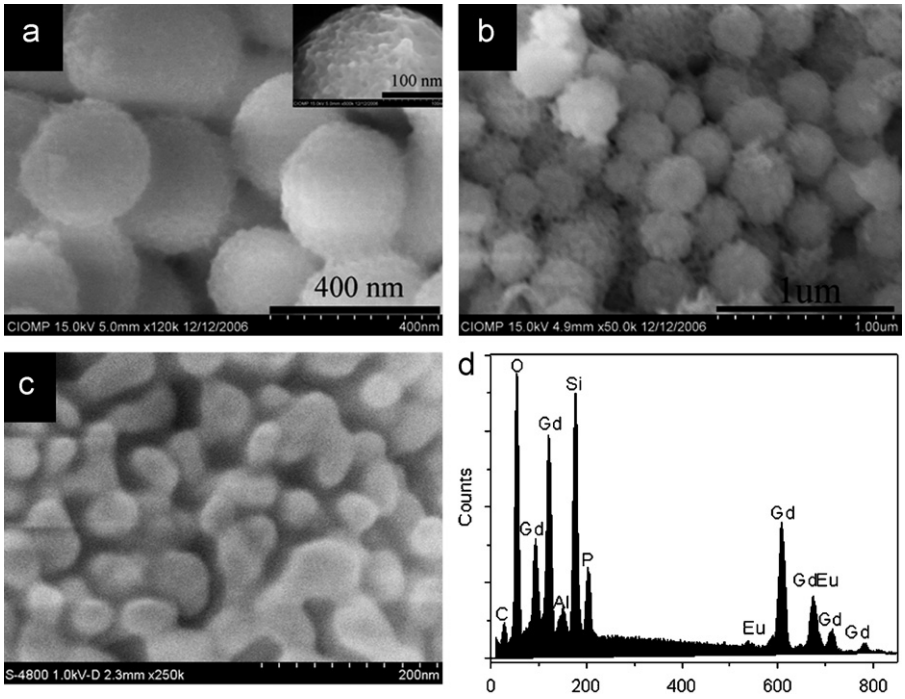

Fig. 2. SEM images of Gd_3PO_7:Eu^{3+} nanospheres: (a) as-prepared sample with low magnification; inset: high magnification; (b) annealed sample with low magnification; (c) annealed sample with high magnification; (d) EDX spectrum of Gd_3PO_7:Eu^{3+} nanospheres.

from a single nanosphere, which further affirms the formation of the Gd_3PO_7 phase. In the EDX spectrum, the strong Si peak came from the Si substrate of the sample.

3.2. Photoluminescence characterization

Annealed Gd_3PO_7:Eu^{3+} nanospheres exhibit much stronger red emission than the as-prepared sample under the ultraviolet irradiation of 254 nm, as shown in Fig. 3. The main peak at 614 nm originates from the $^5D_0 \rightarrow {}^7F_2$ transition of Eu^{3+}. It implies that the defect of the crystallite is less in the annealed sample, that is, the crystallite is perfect during the annealing process.

The luminescence property of a phosphor material is determined by the electronic structure of luminescence centers in it, and the electronic structure is closely related to the crystal structure of the material. For the luminescence of a europium ion, the $^5D_0 \rightarrow {}^7F_1$ transition is magnetic-dipole-allowed and its intensity is almost independent of the local environment of the Eu^{3+} ion; the $^5D_0 \rightarrow {}^7F_2$ transition is electric-dipole-allowed and its intensity is sensitive to the local structure around the Eu^{3+} ion. The intensity ratio of the $^5D_0 \rightarrow {}^7F_2$ transition to the $^5D_0 \rightarrow {}^7F_1$ transition depends strongly on the local symmetry of the Eu^{3+} site. Therefore, europium ions are often used as probes to detect local environments in a matrix. The annealed sample has the higher ratio of 4.3, and the as-prepared sample has the ratio of 2.8. It reveals that the emission from the annealed sample is pure red than that from the as-prepared sample. The $^5D_0 \rightarrow {}^7F_2$ transition

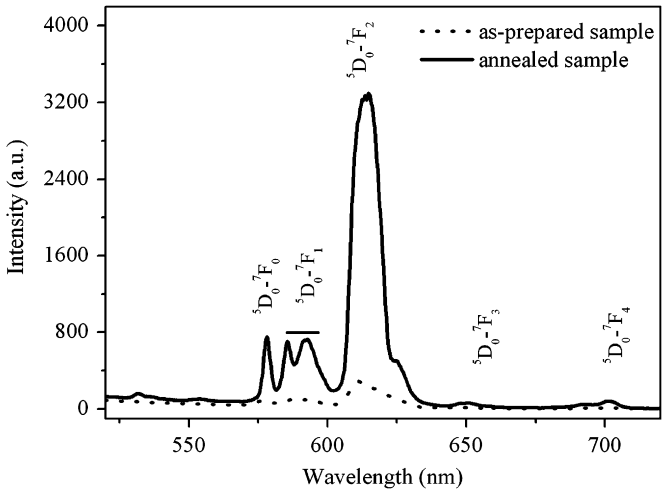

Fig. 3. Room-temperature emission spectra ($\lambda_{ex} = 254$ nm) of Gd_3PO_7:Eu^{3+} nanospheres.

is stronger than the $^5D_0 \rightarrow {}^7F_1$ transition, which indicates that the dopant Eu^{3+} ions mainly occupied non-centrosymmetry sites.

The excitation spectra of the $^5D_0 \rightarrow {}^7F_2$ transition are presented in Fig. 4. A charge transfer band (CTB) can be found in the range of 220–300 nm for both the as-prepared sample and the annealed sample, which is originated from the transition of $2p$ orbital of O^{2-} to the $4f$ orbital of Eu^{3+}. The peak at 206 nm is associated with the host absorption of Gd–O [8]. After annealing, the CTB peak was observed to shift redward by 17 nm, from 258 to 275 nm. CTB is often influenced by nanoscale effect and some interesting

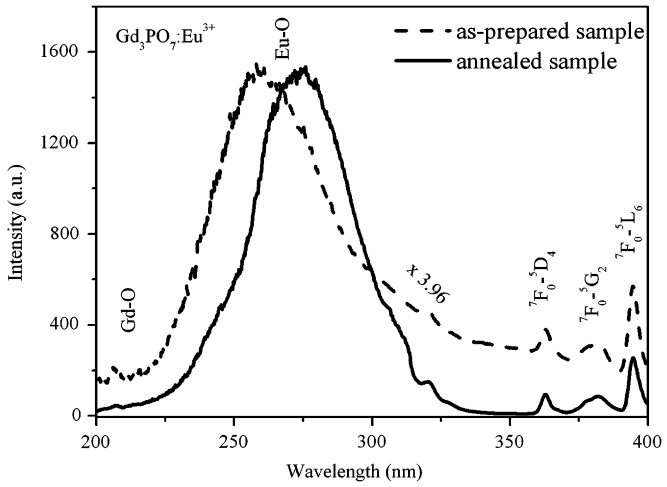

Fig. 4. Excitation spectra ($\lambda_{em} = 614$ nm) of Gd_3PO_7:Eu^{3+} nanospheres for the as-prepared sample and the annealed sample.

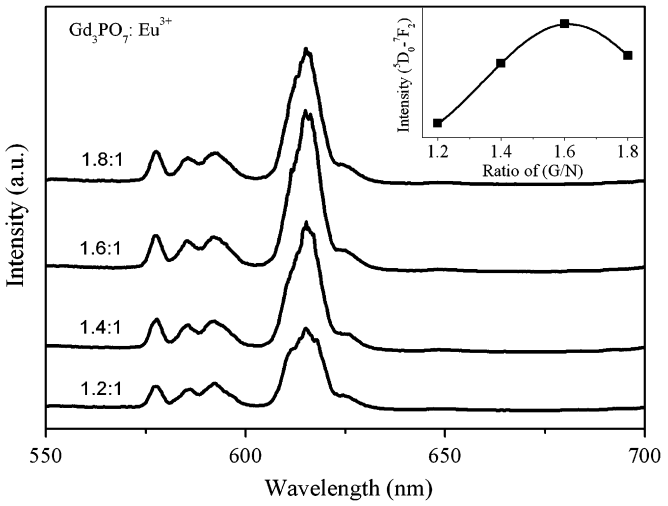

Fig. 5. Emission spectra of Gd_3PO_7:Eu^{3+} nanospheres with different glycin-to-nitrate ratios. Inset: dependence of luminescence intensity of the $^5D_0 \rightarrow {}^7F_2$ transition on the glycin-to-nitrate ratio.

phenomena have been observed as the particle size changes [15–21]. Igarashi et al. [21] reported that the CTB in Y_2O_3:Eu^{3+} nanocrystallites had a blue shift, which was assigned to the decrease of crystal size and agreed with our observation. In oxides, the position of a CTB usually depends on the bond length of Eu–O and the coordination environment around Eu^{3+} [20]. During annealing, the crystal field around Eu^{3+} changed and caused the CTB to shift, as observed in the spectra.

Fig. 5 depicts the dependence of luminescence intensity on the glycin-to-nitrate ratio. The intensity of the $^5D_0 \rightarrow {}^7F_2$ transition increased with the ratio varying from 1.2:1 to 1.8:1 and reached the maximum at 1.6:1, as shown in the inset. It interprets that the more the glycin, the better the combustion when the glycin-to-nitrate ratio is lower than 1.6:1; and while the ratio is increased further, excessive glycin is noxious for the luminescence.

3.3. CIE1931 XY chromaticity coordinate of Gd_3PO_7:Eu^{3+}

In annealed Gd_3PO_7:Eu^{3+} nanospheres, the intensity of the $^5D_0 \rightarrow {}^7F_2$ transition is stronger than those of other $^5D_0 \rightarrow {}^7F_j$ ($j = 0, 1, 3, 4$), which is advantageous to obtain good CIE1931 chromaticity coordinates for a red phosphor. The CIE values for Gd_3PO_7:Eu^{3+} nanospheres are calculated to be $x = 0.654$, $y = 0.345$ (the calculation process is shown in the Supporting Information), which are in the red area close to the National Television Standard Committee (NTSC) standard values for red ($x = 0.670$, $y = 0.330$) and better than those of Y_2O_3:Eu^{3+} phosphor [21].

3.4. Temperature dependence of $^5D_0 \rightarrow {}^7F_2$ emission

Under 325-nm laser excitation, emission spectra of the annealed sample were recorded at different temperatures (Fig. 6) and the photoluminescence intensity of the $^5D_0 \rightarrow {}^7F_2$ transition as a function of temperature is drawn out by joining up the dots in Fig. 8. The intensity increased

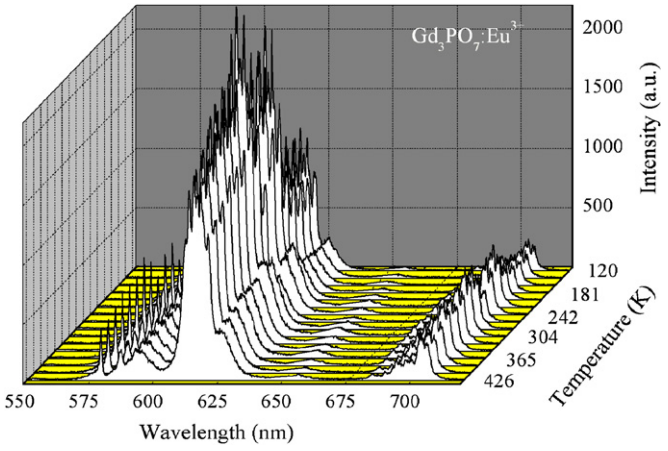

Fig. 6. Emission spectra at various temperatures under 325-nm He–Cd laser excitation.

slowly from 150 to 225 K and quickly from 225 to 304 K and reached the maximum at the room temperature of ~304 K. Then it decreased quickly from 304 to 360 K and slowly from 360 to 426 K. Comparing the intensity at 426 K with the maximum, we found that the intensity decreased by 29.3%. Therefore, the optimal temperature for this material as a red phosphor is 304 K, about room temperature.

The influencing mechanism of temperature on red emission is complicated in Gd_3PO_7:Eu^{3+} nanospheres. Under 325-nm excitation, which is in resonance with the $^7F_2 \rightarrow {}^5L_6$ transition of Eu^{3+} ions, there are two main contributions leading the 614-nm luminescence to change with the elevated temperature. One is the thermal-activated distribution of Eu^{3+} ions in ^7F_J ($J = 0, 1, 2$) states. Eu^{3+} ions in the $^7F_0$ state can be thermally activated to the nearby $^7F_1$ and $^7F_2$. The other contribution is that Eu^{3+}

ions in $^7F_0$ and $^7F_1$ are nonresonantly excited to $^5L_6$ with the assistance of phonons. As the temperature is high enough, multi-phonon-assisted absorption occurs. These two processes may cause the luminescence intensity of the $^5D_0 \rightarrow {}^7F_2$ transition to increase with increasing temperature. Meanwhile, the temperature-quenching effect of Eu^{3+} luminescence becomes strong with the elevated temperature, which is generally caused by nonradiative transition and energy transfer processes. The temperature-quenching channels include the main nonradiative transitions from $^5L_6 \rightarrow {}^5D_0$ and the energy transfer from one activated center Eu^{3+} to the other or to the defect center. This is the main reason leading the luminescence intensity of the $^5D_0 \rightarrow {}^7F_2$ transition to decrease with the elevated temperature. These two processes explain the appearance of a maximum in the temperature dependence of Fig. 7.

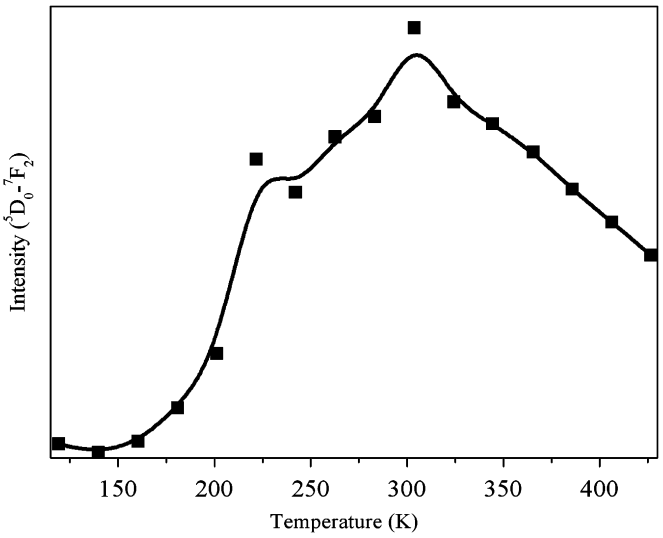

Fig. 7. Dependence of emission intensity of the $^5D_0 \rightarrow {}^7F_2$ transition on temperature.

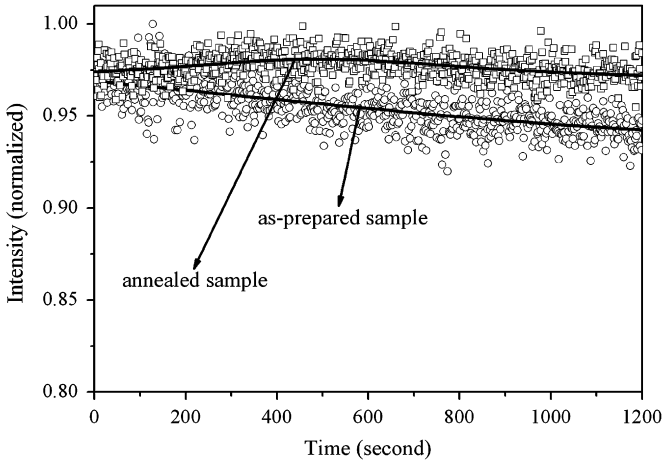

Fig. 8. Dependence of the $^5D_0 \rightarrow {}^7F_2$ transition intensity on the time of 254-nm irradiation for the as-prepared sample and the annealed sample.

3.5. Photoluminescence stability

To study the photostability of the samples as phosphors, their spectral changes induced by ultraviolet (254 nm) irradiation were also investigated. Fig. 8 shows the dependence of 614-nm intensity on irradiation time for the samples under the same conditions. The relative intensity of the as-prepared sample is lower than the other and keeps on decreasing. The intensity of the annealed nanospheres increases first and then decreases, but the relative change of the annealed nanospheres is smaller than that of the bulk. It indicates that the annealed nanospheres have better photostability.

4. Conclusions

Pure red-emission phosphor $Gd_3PO_7:Eu^{3+}$ nanospheres have been obtained using a facile combustion method for the first time. The optimal sample as a red phosphor is the annealed one with the glycin-to-nitrate ratio of 1.6:1, which proved to have better photostability under ultraviolet excitation. We present an investigation on the synthesis of $Gd_3PO_7:Eu^{3+}$ nanospheres and their luminescent properties. Its CIE1931 XY chromaticity coordinates are in the red area, near NTSC standard values for red, and the color saturation is better than that of $Y_2O_3:Eu^{3+}$. The preliminary results confirm that it is a pure-color potential phosphor for PDPs and Xe-based mercury-free lamps and the combustion method is in favorable to industrial production. It is also noteworthy that our results are mainly for phosphors of nanometer size, which can be a reference to future studies on nanometer phosphors.

Acknowledgment

The work was supported by the National Natural Science Foundation of China (Grants 10474096 and 50672030).

Appendix A. Supporting information

Supplementary data associated with this article can be found in the online version at doi:10.1016/j.jssc.2008.01.013.

References

[1] Y.X. Pan, Q. Su, H.F. Xu, T.H. Chen, W.K. Ge, C.L. Yang, M.M. Wu, J. Solid State Chem. 174 (2003) 69–73.
[2] D. Haranath, H. Chander, P. Sharma, S. Singh, Appl. Phys. Lett. 89 (2006) 173118–173120.
[3] D. Haranath, H. Chander, N. Bhalla, P. Sharma, K.N. Sood, Appl. Phys. Lett. 86 (2005) 201904–201906.
[4] G. Wakefield, E. Holland, P.J. Dobson, J.L. Hutchison, Adv. Mater. 13 (2001) 1557–1560.
[5] Z.H. Li, J.H. Zeng, Y.D. Li, Small 3 (2007) 438–443.
[6] W.K. Tracy, L.D. Anthony, A.D. Tuan, Chem. Mater. 18 (2006) 3130–3136.

[7] Z.G. Wei, L.D. Sun, C.S. Liao, C.H. Yan, S.H. Huang, Appl. Phys. Lett. 80 (2002) 1447–1449.
[8] X.Q. Zeng, G.Y. Hong, H.P. You, X.Y. Wu, C.H. Kim, C.H. Pyun, B.Y. Yu, H.S. Bae, C.H. Park, I.E. Kwon, Chin. Phys. Lett. 18 (2001) 690–691.
[9] M.I. Martinez-Rubio, T.G. Ireland, G.R. Fern, J. Silver, M.J. Snowden, Langmuir 17 (2001) 7145–7149.
[10] H. Wang, C.K. Lin, X.M. Liu, J. Lin, M. Yu, Appl. Phys. Lett. 87 (2005) 181907–181909.
[11] W.L. Fan, X.Y. Song, S.X. Sun, X. Zhao, J. Solid State Chem. 180 (2007) 284–290.
[12] R.J. Nikhil, G. Latha, J.M. Catherine, Adv. Mater. 13 (2001) 1389–1393.
[13] M.C. Hsu, I.C. Leu, Y.M. Sun, M.H. Hon, J. Solid State Chem. 179 (2006) 1421–1425.
[14] Y. Tao, G.W. Zhao, W.P. Zhang, S.D. Xia, Mater. Res. Bull. 32 (1997) 501–506.
[15] B.M. Tissue, Chem. Mater. 10 (1998) 2837–2845.
[16] L.D. Sun, C.H. Yan, C.S. Liao, C.X. Liu, D. Li, J.Q. Yu, J. Alloys Compd. 275–277 (1998) 234–237.
[17] Y.H. Tseng, B.C. Chiou, C.C. Peng, L. Ozawa, Thin Solid Films 330 (1998) 173–177.
[18] T. Kim, Y. Yoon, D. Kil, Y. Hwang, H. Chung, I. Hoe Kim, Y. Ahn, Mater. Lett. 47 (2001) 290–296.
[19] T. Igarashi, M. Ihara, T. Kusunoki, K. Ohno, T. Isobe, M. Senna, Appl. Phys. Lett. 76 (2000) 1549–1551.
[20] H.E. Hoefdraad, J. Solid State Chem. 15 (1975) 175–177.
[21] W.N. Wang, W. Widiyastuti, O. Takashi, L.I. Wuled, O. Kikuo, Chem. Mater. 19 (2007) 1723–1730.